

Edge states of graphene wrinkles in single-layer graphene grown on Ni(111) F

Cite as: Appl. Phys. Lett. **109**, 143103 (2016); <https://doi.org/10.1063/1.4963858>

Submitted: 01 June 2016 . Accepted: 23 August 2016 . Published Online: 03 October 2016

Liwei Liu, Wende Xiao , Dongfei Wang, Kai Yang, Lei Tao, and Hong-Jun Gao

COLLECTIONS

F This paper was selected as Featured



View Online



Export Citation



CrossMark

ARTICLES YOU MAY BE INTERESTED IN

[Hierarchy of graphene wrinkles induced by thermal strain engineering](#)

Applied Physics Letters **103**, 251610 (2013); <https://doi.org/10.1063/1.4857115>

[Unveiling carbon dimers and their chains as precursor of graphene growth on Ru\(0001\)](#)

Applied Physics Letters **109**, 131604 (2016); <https://doi.org/10.1063/1.4963283>

[Quasi-free-standing graphene nano-islands on Ag\(110\), grown from solid carbon source](#)

Applied Physics Letters **110**, 213107 (2017); <https://doi.org/10.1063/1.4984093>



Your Qubits. Measured.

Meet the next generation of quantum analyzers

- Readout for up to 64 qubits
- Operation at up to 8.5 GHz, mixer-calibration-free
- Signal optimization with minimal latency

Find out more



Edge states of graphene wrinkles in single-layer graphene grown on Ni(111)

Liwei Liu, Wende Xiao,^{a)} Dongfei Wang, Kai Yang, Lei Tao, and Hong-Jun Gao
Institute of Physics, Chinese Academy of Sciences, P.O. Box 603, Beijing 100190, China

(Received 1 June 2016; accepted 23 August 2016; published online 3 October 2016)

As quasi-one-dimensional (1D) structures with characteristic widths of nanometer scale, graphene wrinkles (GWs) have been widely observed in graphene grown by chemical vapor deposition. Similar to conventional 1D graphene-based nanostructures, e.g., carbon nanotubes and graphene nanoribbons, 1D electron confinement has been observed in the GWs. However, it remains an open question whether the GWs have effective edges and exhibit corresponding edge states. Here, we report on the edge states of the GWs in single-layer graphene grown on Ni(111) by means of low temperature scanning tunneling microscopy and spectroscopy. We show that the GWs are decoupled from the substrate, while the surrounding planar graphene are strongly coupled with the substrate. The different graphene-substrate coupling leads to effective edges and 1D character of the GWs. The chiral edges of the GWs give rise to pronounced edge states around the Fermi level in the density of states. *Published by AIP Publishing.* [<http://dx.doi.org/10.1063/1.4963858>]

The epitaxial growth and electronic structures of graphene on transition metal substrates have attracted intense interest within a decade after the discovery of graphene flakes by mechanical exfoliation,^{1–16} driven by the unique opportunities to fabricate large-area uniform graphene layers with low defect density, which is crucial for applications in future devices. However, graphene wrinkles (GWs), which are essentially bended graphene structures that are chemically bonded with surrounding planar graphene (PG), often exist in graphene grown by chemical vapor deposition, due to the different thermal expansion coefficients of graphene and metal substrates.^{17–25} Although a GW is still a part of the continuous two-dimensional (2D) graphene, it can be viewed as a quasi-one-dimensional (1D) structure,²⁵ due to its unique geometrical shape. Thus, the GWs might exhibit intriguing 1D electronic properties and influence the transport properties of graphene.^{23,25} Recently, Lim *et al.* studied the electron confinement in GWs by scanning tunneling microscopy and spectroscopy (STM/STS) and observed a 1D van Hove singularity (VHS) in the GWs in a graphene sheet grown on Ni(111).²⁵ However, a GW is distinct from other conventional 1D graphene-based nanostructures, e.g., graphene nanoribbons (GNRs) and carbon nanotubes (CNTs): A GNR has two edges, but a CNT has none. This raises an interesting question: Does a GW have effective edges and exhibit corresponding edge states?

In this work, we report on the edge states of the GWs in single-layer graphene grown on Ni(111) by means of STM/STS. We show that the GWs are decoupled from the substrate, while the surrounding PG is strongly coupled with the substrate. The different graphene-substrate coupling leads to effective edges and 1D character of the GWs. The chiral edges of the GWs give rise to pronounced edge states around the Fermi level (E_F) in the density of states (DOS) of the GWs.

The experiments were carried out in an ultrahigh vacuum (base pressure of 1×10^{-10} mbar) low temperature

STM system (Unisoku), equipped with standard surface preparation facilities including an ion sputtering gun and electron-beam heater for surface cleaning. The Ni(111) surface was cleaned by repeated cycles of ion sputtering using Ar^+ with an energy of 1.5 keV, annealing at 600 °C, and oxygen exposure at 400 °C (5×10^{-7} mbar, 5 min). Prior to the growth of graphene, the surface cleaning of the Ni(111) substrate was checked by low energy electron diffraction and STM. Single-layer graphene was obtained via pyrolysis of ethylene on a Ni(111) substrate that was held at 800 °C.²⁴ STM images were acquired in the constant-current mode. Differential conductance (dI/dV) spectra were collected by using a lock-in technique with a 0.5 mV_{rms} sinusoidal modulation at a frequency of 973 Hz. All STM/STS experiments were performed with electrochemically etched tungsten tips at 4.3 K, which were calibrated with respect to the Au(111) surface state before and after spectroscopic measurements. The given voltages were referred to the sample.

Figure 1(a) shows a large-scale STM image of the as-prepared single-layer graphene on Ni(111). The GWs indicated by the white arrows appear as 1D protrusions across the flat terraces that are covered by planar single-layer graphene. No moiré pattern is observed on the PG. Figure 1(b) displays a zoom-in on such a flat graphene region. A honeycomb lattice is clearly resolved. These behaviors indicate that the PG exhibits a 1×1 structure with respect to the Ni(111) lattice, due to a nearly perfect matching between the graphene and Ni(111) lattices, in line with previous reports.^{12–14,24,26} dI/dV spectra acquired on the PG exhibit a sharp peak at about -125 mV and a broad peak in the range of 50 mV to 200 mV, as shown in Fig. 1(c). This feature of dI/dV spectra is distinct from the V-shaped DOS near the Fermi level for free-standing graphene, suggesting that the electronic structure of graphene has been significantly altered due to the graphene-substrate interaction. Previous density functional theory (DFT) calculations based on the 1×1 structure of graphene on Ni(111) reveal a distance of ~ 2.1 Å between the graphene overlayer and the Ni(111) surface and a strong coupling between graphene and the

^{a)} Author to whom correspondence should be addressed. Electronic mail: wdxiao@iphy.ac.cn. Tel.: +86-10-82648048. Fax: +86-10-62556598.

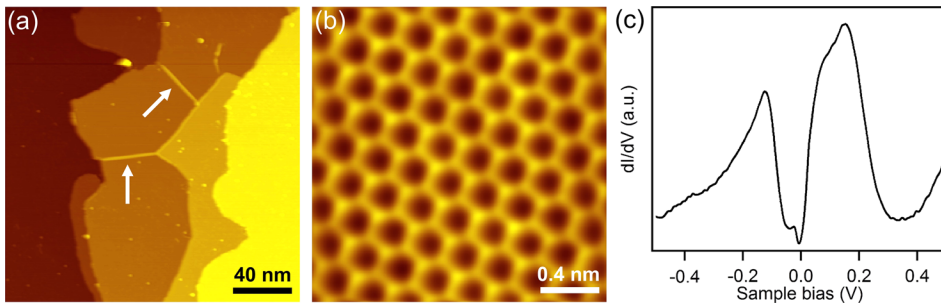


FIG. 1. (a) Large-scale STM image showing the formation of GWs in single-layer graphene grown on Ni(111) (sample bias: $U = -200$ mV; tunneling current: $I = 10$ pA). (b) Atomic-resolution image acquired on PG showing a honeycomb lattice ($U = -20$ mV, $I = 190$ pA). This image has been filtered. (c) dI/dV spectrum acquired on PG (setpoint: $U = -200$ mV, $I = 140$ pA).

substrate.^{27–29} Recently, Garcia-Lekue and coworkers reported similar dI/dV spectra for graphene grown on Ni(111).³⁰ They assigned the sharp peak at about -125 mV and the broad peak in the range of 50 mV to 200 mV to the majority and minority states of graphene/Ni, respectively, according to the calculated spin-polarized DOS projected onto carbon atoms.³⁰ The π -electrons of graphene are strongly hybridized with the spin-polarized free electrons of the Ni(111) substrate.^{30,31} Notably, the dI/dV spectra collected on graphene/Ni(111) by Lim *et al.* display no significant peak in the vicinity of E_F .²⁵

After clarifying the electronic structures of the PG, let us turn to the structural and electronic properties of the GWs. Figure 2(a) shows a three-dimensional (3D) STM topography image of a GW on a flat terrace of Ni(111). Line profile analysis (Fig. 2(b)) reveals a width of ~ 3.5 nm and a height of ~ 0.28 nm. These values are rather small compared to the length of ~ 30 nm (Fig. 2(a)), evidencing a 1D geometry of the GW. The atomically resolved STM image (Fig. 2(c)) illustrates that this GW is seamlessly connected with the PG. The carbon atoms of the GW are better resolved than the ones assigned to the surrounding PG, indicating that the GW is decoupled from the Ni substrate. This atomic-resolution image is slightly distorted, as it is essentially an image of the bended GW projected on a plane. The edges of

the GW can be clearly seen, which is neither zigzag nor arm-chair but a general chiral edge. According to the method reported in the previous work,^{25,34} this chiral edge can be described by an index of (4, 1). Figure 2(d) illustrates a schematic model of graphene on Ni(111) with a GW, showing that the GW can be viewed as a GNR due to the different graphene-substrate binding in the GW and planar graphene regions. The 1D geometry and the presence of effective edges are expected to result in unique electronic structures in the GWs.

To explore its electronic structures, we have measured dI/dV spectra across the GW shown in Fig. 2(c). Figure 3 displays a series of dI/dV spectra collected at different sites across the GW shown in Fig. 2(c). The dI/dV spectrum (red curve) acquired at the center of the GW exhibits a prominent peak at about -0.035 V, a weak peak at about 0.026 V, and two peaks at ± 0.22 V. Similar dI/dV spectra have been collected at different sites across the GW, except that the dI/dV spectrum (green curve) acquired at the edge of the GW exhibits a mixed feature of that of PG and that of the GW center. These behaviors indicate that the electronic structure of the GW is distinct from that of PG, due to the decoupling of the GW from the substrate. Meanwhile, the dI/dV spectra

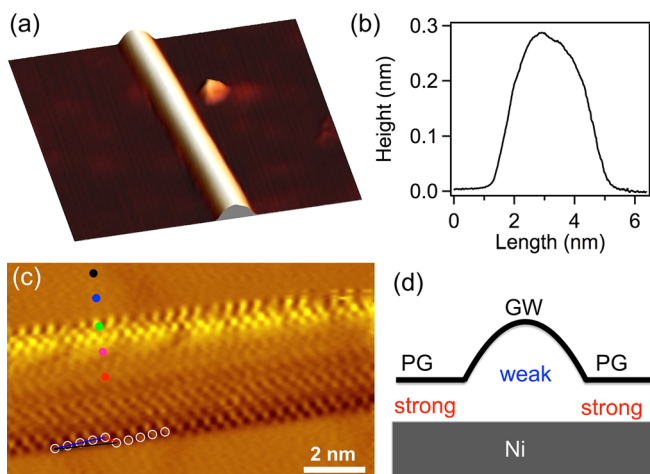


FIG. 2. (a) 3D STM image of a GW on a flat terrace of the Ni(111) surface ($U = -110$ mV, $I = 120$ pA). (b) Line profile showing that the GW has a width of ~ 3.5 nm and a height of ~ 0.28 nm. (c) Derivative image showing the atomic structure of the GW shown in (a) ($U = -180$ mV, $I = 90$ pA). This image has been filtered to enhance the contrast. The C atoms of a section of an effective edge are indicated by white cycles. The projections of the (4, 1) vector onto the basis vectors of the graphene lattice are represented by the blue and red lines. (d) Schematic model of a GW on Ni(111) showing the different graphene-substrate coupling for the GW and PG.

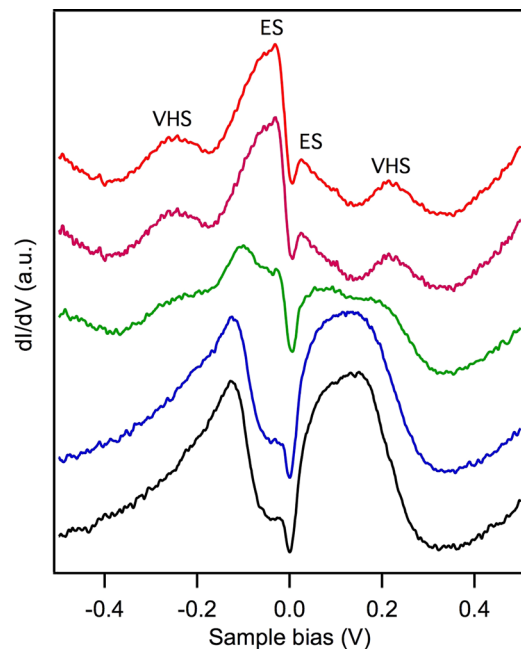


FIG. 3. dI/dV spectra acquired at different sites across the GW indicated by colored dots shown in Fig. 2(c). The curves are offset vertically for clarity. The prominent peak at -0.035 V and the weak peak at 0.026 V are assigned to the spin-split edge states, while the two peaks at ± 0.22 eV are attributed to the VHS states.

collected along the GW (not shown) exhibit a similar feature but different from the V-shaped DOS of free-standing graphene, suggesting that the 1D geometry of the GW is of great importance for its intriguing electronic structures. We assign the two weak peaks located at ± 0.22 eV to the VHS states, which always appear in pairs with respect to E_F due to 1D electron confinement.³² We note that the Landau levels induced by strain in the GW can be safely excluded in our work, as the positions of the peaks do not follow the relationship of $E_n \propto \text{sgn}(n)\sqrt{|n|}$ that are expected for the n th Landau levels in single-layer graphene.³³ Lim and coworkers recently studied the electronic structures of the GWs with various widths and chiral edges grown on Ni(111) by STM/STS.²⁵ VHS states were observed for GWs with width < 3.5 nm.²⁵ The measured gap between the VHS in our work is much smaller than that reported by Lim and coworkers, probably due to the larger width of the GW in our work than that in the previous report.

The prominent peak at -0.035 V and the weak peak at 0.026 V in the dI/dV spectra are assigned to the spin-split edge states of the GW, similar to the spin-split edge states observed in GNRs.³⁴ The different intensity of the two spin-polarized peaks might be due to the presence of the Ni substrate, which is spin-polarized and can enhance the peak with the same spin polarization, but suppress the one with the opposite spin polarization. Previous theoretical calculations revealed that a general edge structure that is not parallel to the armchair edge can have zero-energy edge states,^{32,35,36} in line with our observations. Notably, several GWs with different lengths, widths and chiral indices were studied and similar edge states were observed. We note that the edge state around E_F was absent in their dI/dV measurements.²⁵

In summary, we have investigated the structural and electronic properties of GWs in single-layer graphene grown on the Ni(111) surface by LT-STM/STS. The GWs are decoupled from the Ni(111) substrate, in contrast to the strong coupling between the PG and the Ni substrate. The different graphene-substrate coupling leads to effective edges and 1D character of the GWs. The chiral edges of the GWs give rise to pronounced edge states around the E_F in the DOS, resulting in a metallic feature. Moreover, the 1D confinement of electrons leads to the appearance of VHS states in the GWs. As GWs have been widely observed for graphene epitaxially grown various metal substrates, similar edge states are expected for the GWs and might exert significant impact on the transport properties of the epitaxial graphene.

The work was financially supported by grants from MOST (No. 2015CB921103), NSFC (No. 61574170) and CAS in China.

¹K. S. Novoselov, A. K. Geim, S. V. Morozov, D. Jiang, Y. Zhang, S. V. Dubonos, I. V. Grigorieva, and A. A. Firsov, *Science* **306**, 666 (2004).

²Y. B. Zhang, Y. W. Tan, H. L. Stormer, and P. Kim, *Nature* **438**, 201 (2005).

³A. H. Castro Neto, F. Guinea, N. M. R. Peres, K. S. Novoselov, and A. K. Geim, *Rev. Mod. Phys.* **81**, 109 (2009).

- ⁴S. Das Sarma, S. Adam, E. H. Hwang, and E. Rossi, *Rev. Mod. Phys.* **83**, 407 (2011).
- ⁵Y. Pan, D. X. Shi, and H. J. Gao, *Chin. Phys.* **16**, 3151 (2007).
- ⁶S. Marchini, S. Gunther, and J. Wintterlin, *Phys. Rev. B* **76**, 075429 (2007).
- ⁷P. W. Sutter, J. I. Flege, and E. A. Sutter, *Nat. Mater.* **7**, 406 (2008).
- ⁸Y. Pan, H. G. Zhang, D. X. Shi, J. T. Sun, S. X. Du, F. Liu, and H. J. Gao, *Adv. Mater.* **21**, 2777 (2009).
- ⁹J. Wintterlin and M. L. Bocquet, *Surf. Sci.* **603**, 1841 (2009).
- ¹⁰A. T. N'Diaye, S. Bleikamp, P. J. Feibelman, and T. Michely, *Phys. Rev. Lett.* **97**, 215501 (2006).
- ¹¹H. Ueta, M. Saida, C. Nakai, Y. Yamada, M. Sasaki, and S. Yamamoto, *Surf. Sci.* **560**, 183 (2004).
- ¹²M. Gao, Y. Pan, C. D. Zhang, H. Hu, R. Yang, H. L. Lu, J. M. Cai, S. X. Du, F. Liu, and H.-J. Gao, *Appl. Phys. Lett.* **96**, 053109 (2010).
- ¹³Yu. S. Dedkov, M. Fonin, U. Rüdiger, and C. Laubschat, *Phys. Rev. Lett.* **100**, 107602 (2008).
- ¹⁴A. Varykhalov, J. Sánchez-Barriga, A. M. Shikin, C. Biswas, E. Vescovo, A. Rybkin, D. Marchenko, and O. Rader, *Phys. Rev. Lett.* **101**, 157601 (2008).
- ¹⁵X. S. Li, W. W. Cai, J. H. An, S. Kim, J. Nah, D. X. Yang, R. Piner, A. Velamakanni, I. Jung, E. Tutuc, S. K. Banerjee, L. Colombo, and R. S. Ruoff, *Science* **324**, 1312 (2009).
- ¹⁶L. Gao, J. R. Guest, and N. P. Guisinger, *Nano Lett.* **10**, 3512 (2010).
- ¹⁷S. J. Chae, F. Güneş, K. K. Kim, E. S. Kim, G. H. Han, S. M. Kim, H.-J. Shin, S.-M. Yoon, J.-Y. Choi, M. H. Park, C. W. Yang, D. Pribat, and Y. H. Lee, *Adv. Mater.* **21**, 2328 (2009).
- ¹⁸H. Cao, Q. Yu, R. Colby, D. Pandey, C. S. Park, J. Lian, D. Zemlyanov, I. Childres, V. Drachev, E. A. Stach, M. Hussain, H. Li, S. S. Pei, and Y. P. Chen, *J. Appl. Phys.* **107**, 044310 (2010).
- ¹⁹K. Kim, Z. Lee, B. D. Malone, K. T. Chan, B. Alemán, W. Regan, W. Gannett, M. F. Crommie, M. L. Cohen, and A. Zettl, *Phys. Rev. B* **83**, 245433 (2011).
- ²⁰Y. Zhang, T. Gao, Y. Gao, S. Xie, Q. Ji, K. Yan, H. Peng, and Z. Liu, *ACS Nano* **5**, 4014 (2011).
- ²¹T. M. Paronyan, E. M. Pigos, G. Chen, and A. R. Harutyunyan, *ACS Nano* **5**, 9619 (2011).
- ²²H. Hattab, H. Hattab, A. T. N'Diaye, D. Wall, C. Klein, G. Jnawali, J. Coraux, C. Busse, R. van Gastel, B. Poelsema, T. Michely, F.-J. Meyer zu Heringdorf, and M. Horn-von Hoegen, *Nano Lett.* **12**, 678 (2012).
- ²³W. Zhu, T. Low, V. Perebeinos, A. A. Bol, Y. Zhu, H. Yan, J. Tersoff, and P. Avouris, *Nano Lett.* **12**, 3431 (2012).
- ²⁴J. Lahiri, Y. Lin, P. Bozkurt, I. I. Oleynik, and M. Batzill, *Nat. Nanotechnol.* **5**, 326 (2010).
- ²⁵H. Lim, J. Jung, R. S. Ruoff, and Y. Kim, *Nat. Commun.* **6**, 8601 (2015).
- ²⁶M. Olle, G. Ceballos, D. Serrate, and P. Gambardella, *Nano Lett.* **12**, 4431 (2012).
- ²⁷J. Maassen, W. Ji, and H. Guo, *Nano Lett.* **11**, 151 (2011).
- ²⁸V. M. Karpan, G. Giovannetti, P. A. Khomyakov, M. Talanana, A. A. Starikov, M. Zwierzycki, J. van den Brink, G. Brocks, and P. J. Kelly, *Phys. Rev. Lett.* **99**, 176602 (2007).
- ²⁹F. Mittendorfer, A. Garhofer, J. Redinger, J. Klimeš, J. Harl, and G. Kresse, *Phys. Rev. B* **84**, 201401(R) (2011).
- ³⁰A. Garcia-Lekue, T. Balashov, M. Olle, G. Ceballos, A. Arnau, P. Gambardella, D. Sanchez-Portal, and A. Mugarza, *Phys. Rev. Lett.* **112**, 066802 (2014).
- ³¹Y. Murata, V. Petrova, B. B. Kappes, A. Ebnonnasir, I. Petrov, Y.-H. Xie, C. V. Ciobanu, and S. Kodambaka, *ACS Nano* **4**, 6509 (2010).
- ³²K. Wakabayashi, K.-i. Sasaki, T. Nakanishi, and T. Enoki, *Sci. Technol. Adv. Mater.* **11**, 054504 (2010).
- ³³N. Levy, S. A. Burke, K. L. Meaker, M. Panlasigui, A. Zettl, F. Guinea, A. H. Castro Neto, and M. F. Crommie, *Science* **329**, 544 (2010).
- ³⁴C. Tao, L. Jiao, O. V. Yazyev, Y.-C. Chen, J. Feng, X. Zhang, R. B. Capaz, J. M. Tour, A. Zettl, S. G. Louie, H. Dai, and M. F. Crommie, *Nat. Phys.* **7**, 616 (2011).
- ³⁵M. Wimmer, A. R. Akhmerov, and F. Guinea, *Phys. Rev. B* **82**, 045409 (2010).
- ³⁶K. Wakabayashi, Y. Takane, M. Yamamoto, and M. Sigrist, *Carbon* **47**, 124 (2009).